High-resolution simulations of freely decaying shallow-water turbulence on a rotating sphere (*)(**)

R. IACONO (1)(***), M. V. STRUGLIA (1), C. RONCHI (2) and S. NICASTRO (1)
(1) *ENEA - C.R. Casaccia, Gruppo di Dinamica Atmosferica e Oceanica*
V. Anguillarese 301, 00060 S. Maria di Galeria, Roma, Italy
(2) *Via Flaminia 357, 00196 Roma, Italy*

(ricevuto il 18 Novembre 1998; approvato il 6 Maggio 1999)

Summary. — Results of high-resolution, long-time numerical integrations of the unforced shallow-water equations on a rotating sphere are presented. A new accurate and efficient grid point method is used for these simulations, that allows to easily reach very high spatial resolutions (up to an equivalent T680 spectral truncation). It is found that, for small values of the Rossby deformation radius L_D, the final quasi-steady states of the free evolution are characterized by the formation of robust westward (retrograde) equatorial jets, whose strengths and widths depend on L_D and on the rotation speed. It is also shown that the presence of a westward equatorial jet is related to the global prevalence of anticyclonic vorticity.

PACS 92.10.Lq – Turbulence and diffusion.
PACS 92.60.Bh – General circulation.
PACS 47.27.Eq – Turbulence simulation and modeling.
PACS 01.30.Cc – Conference proceedings.

1. – Introduction

A large body of literature, steadily growing in the last twenty years, has been devoted to the theoretical and computational investigation of incompressible two-dimensional (2D) turbulence in planar geometry. Many of these works have dealt with the emergence of coherent structures, such as vortices and jets, both in forced and in freely decaying situations. More recently, in the attempt of increasing the relevance to the dynamics of planetary atmospheres, more complex physical models have been considered, and, in few cases, spherical geometry has been used, instead of local projections on tangent planes (the so-called f and β planes). Results of high-resolution numerical simulations of incompressible 2D turbulence on a rotating sphere have been presented in ref. [1], where the attention was focused on the role of rotation in the

(*) Paper presented at the International Workshop on "Vortex Dynamics in Geophysical Flows", Castro Marina (LE), Italy, 22-26 June 1998.
(**) The authors of this paper have agreed to not receive the proofs for correction.
(***) E-mail: roberto@mantegna.casaccia.enea.it

spontaneous emergence of circumpolar vortices, and in ref. [2], where external forcing was used to produce banded structures in potential vorticity. Some analytical and numerical studies (see, for example, [3]) in Cartesian geometry have used quasi-geostrophic models obtained by asymptotic approximations of the shallow-water equations (SWE), which are the one-layer limit of the underlying primitive equations. A few numerical investigations [4-6] have dealt with shallow-water freely decaying turbulence on the *f*-plane. In ref. [6], in particular, it was shown that the presence of a finite deformation radius, together with rotation, can lead to the breaking of cyclone-anticyclone symmetry, with a prevalence of anticyclones in the final quasi-steady states of the evolution.

The first long-time numerical simulations of shallow-water turbulence on a rotating sphere were performed by Cho and Polvani [7, 8]. No external forcing was used in these studies, since it was argued that, before going to more realistic and complicated models, it is interesting to see how much of the observed behaviour can be captured with a simple unforced model. In fact, even if great care should be used in claiming any direct relation with the real global circulation on planets, which is three-dimensional and driven by thermal effects not included in the model, interesting results were found. For values of the parameters relevant for the Jovian planets, robust equatorial jets emerged spontaneously from random initial conditions, with strengths and latitudinal extents similar to the observed ones, although, in some cases, with wrong directions. In addition, a region of the parameter space was found, in which asymmetry between cyclones and anticyclones developed from a symmetric initial state, favouring anticyclonic structures.

In the present work, we will give a first description of the results of analogous simulations we have performed, together with details of the numerical techniques employed. Instead of standard spectral transform solvers, we have in fact used a SWE solver based on a new grid point method, the "Cubed Sphere" (CS) [9, 10], which is more efficient than the spectral method while preserving a similar accuracy. This allowed us to reach a maximum spatial resolution corresponding to that of a T680 spectral truncation, which is four times higher than the one used in refs. [7, 8].

We concentrated on the study of the equatorial jet characteristics and on their dependence on the non-dimensional parameters of the equations (Rossby and Froude numbers), with results that are in qualitative agreement with those presented in ref. [7]. However, we point out an interesting new feature: the existence of a threshold in Froude number beyond which the equatorial jet is formed, always in the westward direction. We show, both from numerical evidence and from basic properties of two-dimensional flows in spherical geometry, that the emergence of such a jet is a signal of the global prevalence of anticyclonic vorticity on the sphere.

The threshold for jet formation is found to be very close to that given in ref. [7] for the breaking of cyclone-anticyclone symmetry, suggesting a deeper relation between the two phenomena. This aspect is further investigated in a companion paper [11].

The plan of the paper is the following. The CS method is briefly introduced in sect. **2**. In sect. **3**, the physical model and the numerical procedure are outlined. The main results are presented in sect. **4**. Finally, in the last section, conclusions are drawn.

2. – The Cubed Sphere method

The Cubed Sphere method is a new grid point numerical method for solving partial differential equations in spherical geometry. In this method, the spherical surface is

TABLE I. – *Performances of the CSSWM code, at different spatial resolutions.*

	Equivalent spectral truncation	Number of CPUs	Sustained perf. (Gflops)	CPU (h) (Quadrics)	CPU (h) (Cray C90)
C128	T170	128	0.64	3	3.9
C256	T340	512	2.6	7.5	38.2
C512	T680	512	5.2	30	305
C1024	T1360	512	7.8	160	2440

divided into six identical regions, obtained through the central projection of a circumscribed cube. These regions are then covered with grids made by angularly equidistant great circles, which together form a global, non-singular, quasi-uniform grid. The six local grids are coupled together at their boundaries using an interpolation procedure based on a variation of the composite mesh technique [12], which allows to obtain stable and accurate numerical solutions with a minimum amount of overlap equal to the boundary lines between blocks.

The CS method has proven to be as accurate as the spectral transform method, while allowing substantial savings in computing time, thanks to the more favourable scaling of the operation count with resolution [10]. A shallow-water solver has been written, named CSSWM (Cubed Sphere Shallow Water Model), which is based on the CS grid. This solver uses fourth-/sixth-order–centered finite differences in space, third-order Adams-Bashfort [13] for time stepping and explicit $-\Delta^2$, or Δ^3—depending on the order of the finite differencing—hyperdiffusion operators. The CSSWM code has also been efficiently implemented [14] on massively parallel computers of the APE100/Quadrics family [15], with a maximum peak power of 25.6 Gflops. Together with the intrinsic efficiency of the method, this allowed us to use very high spatial resolutions. In fact, we can span from a C64 (meaning that each of the six grids covering the spherical surface has 64×64 grid points) to a C1024, roughly corresponding to a T1360 spectral truncation.

The performances of the CSSWM code on different configurations of the parallel machine are shown in table I, for simulations spanning 560 planetary rotations. As a reference, the computational times on a single CPU of Cray C90 are given in the last column of the table. The corresponding CPU time for the spectral solver, for equal time steps, is about 8 times higher at the lowest resolution, and more than 60 times higher at C1024. This is because, due the Legendre transform part of the spectral algorithm, the ratio of floating point operations per time step between the spectral and the CS solvers increases linearly with resolution (approximately as $0.03N$, where N is the number of latitudes of the underlying Gaussian grid).

3. – The numerical experiments

We solve the SWE in their velocity-height formulation. In non-dimensional form they can be written as

$$\frac{\partial \mathbf{v}}{\partial t} + (\mathbf{v}\cdot\nabla)\,\mathbf{v} = -\frac{1}{F^2}\nabla h - \frac{\sin\theta}{R}\,\hat{k}\times\mathbf{v} + \varepsilon_{\mathbf{v}} D(\mathbf{v})\,, \tag{1}$$

$$\frac{\partial h}{\partial t} + \mathbf{v}\cdot\nabla h = -(1+h)\,\nabla\cdot\mathbf{v} + \varepsilon_h D(h), \tag{2}$$

where $\mathbf{v}$ is the horizontal fluid velocity, h is the characteristic deviation from the mean height H, $\hat{k}$ is the outward radial unit vector, and θ is the latitude. The operator D is a numerical hyperdiffusion operator defined as $(-1)^{p-1}\Delta^p$.

Only two non-dimensional parameters appear in the equations: the Rossby number $\mathrm{Ro} = U/2\Omega L$ and the Froude number $\mathrm{Fr} = U/\sqrt{gH}$. Here g is the gravitational constant, U and L are the characteristic scales of horizontal velocity and length, and Ω is the planetary rotation rate. The values of Ro and Fr of the initial conditions define a two-dimensional parameter space in which the behaviour of the SWE is investigated [6]. The location in the (Ro, Fr)-plane of the set of initial conditions used in the present work is shown in fig. 1, where solid lines approximately delimit the region of validity of the shallow-water equations. Most of the runs were initialized close to the line $\mathrm{Fr}^2/\mathrm{Ro} = 0.13$ (dotted line), that was indicated in ref. [7] as the rough border between evolutions preserving (to the left) or non-preserving the initial symmetry between cyclones and anticyclones.

In this study we have considered initial conditions with different values of Ro and Fr, but with the same shape of the energy spectrum, given by $E(n) \sim n^{\gamma/2}/(n+n_0)^{\gamma}$, where the one-dimensional spectral index n is the index of the associated Legendre functions. The parameters n_0 and γ, controlling the maximum position and the spectrum width, are chosen to be $n_0 = 14$ and $\gamma = 18$ for all runs in fig. 1. Energy is equipartitioned among different m's (Fourier wave numbers), and each mode is multiplied by a random phase. Since the flow is taken to be non-divergent, this completely defines the initial velocity field.

All runs in fig. 1 were made at a C256 resolution. Some were also made at lower (C128) and higher (C512) resolutions, to test the effect of increasing spatial resolution. While some changes in the number, width and amplitude of the zonal jets were

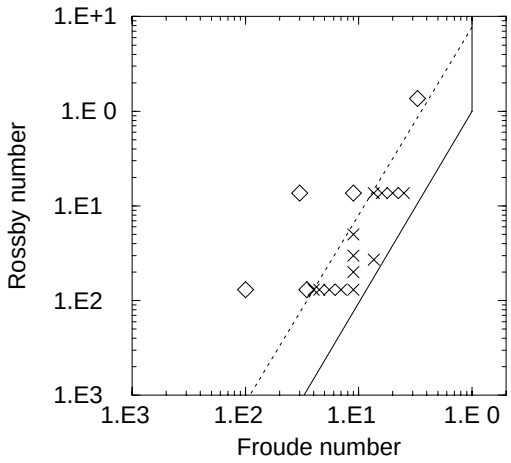

Fig. 1. – The (Ro, Fr) parameter space of the initial conditions. Solid lines approximately delimit the region of validity of the shallow-water equations, while the dashed line corresponds to $\mathrm{Fr}^2/\mathrm{Ro} = 0.13$. Diamonds indicate runs in which the initial symmetry between cyclones and anticyclones is maintained, while crosses mark those runs in which asymmetry was developed.

observed going from to C128 to C256, very little additional change was found by further increasing resolution. Therefore, at least for the scopes of the present investigation, the C256 resolution was found to be adequate. We have used fourth-order spatial finite differencing and hyperdiffusion operators, with a diffusion coefficient ε_v of 10^{-7} for runs at a C128 resolution and 10^{-8} for those at C256. Since h is a smoother field, ε_h was taken to be five times smaller than ε_v [16].

4. – Results

As previously noted, the purpose of the present work is not to perform a systematic exploration of the (Ro, Fr) parameter space, such as the one accomplished in ref. [7], where the relation between the dynamics of SWE and that of simpler models, obtained by taking appropriate limits of the equations, was investigated in a detailed way. We concentrate, instead, on the interesting region in the (Ro, Fr)-plane where the freely evolving shallow-water dynamics can lead to breaking of the cyclone-anticyclone symmetry.

In fig. 1, initial conditions marked with a diamond correspond to runs in which the initial symmetry between cyclones and anticyclones was preserved by the evolution, while crosses designate simulations in which asymmetry was developed, always leading to final quasi-steady states with a prevalence of anticyclonic vorticity. These results are consistent with those presented in [7], and the line $\mathrm{Fr}^2/\mathrm{Ro} = 0.13$ seems indeed to separate "symmetric" and "asymmetric" evolutions. However, crossing this line leads to other important changes in terms of macroscopic physical space features. For example, at high Fr, the evolution of the potential vorticity field q is characterized by the spontaneous formation of banded zonal structures on a broad range of latitudes around the equator, while a few lasting coherent vortices are formed in the polar regions. This is due to the combined effect of differential rotation and of a finite deformation radius $L_D = \sqrt{gH}/2\Omega$, which limits the energy cascade towards larger scales in the meridional direction.

The formation of banded structures in q is reflected in the appearence of zonal jets in the zonal velocity profile. In fig. 2, we plot the steady-state meridional profiles of zonally averaged zonal velocity, for different values of the Rossby parameter, at a fixed value of the Froude number, $\mathrm{Fr} = 0.09$. It can be noted how, for sufficiently high rotation speeds, a robust equatorial jet is formed. Both the amplitude of the equatorial jet and the total number of jets increase with the rotation rate (proportional to 1/Ro). On the other hand, no robust equatorial jet is formed in the simulation with $\mathrm{Ro} = 0.13$, which falls in the symmetric (with respect to the cyclone-anticyclone distribution) region of the (Ro, Fr)-plane.

Results from a different series of runs, at fixed Rossby number, $\mathrm{Ro} = 0.13$, are presented in fig. 3. This figure shows that the amplitude of the equatorial jet is an increasing function of Fr too. Again, no robust equatorial jet is present in the simulations initialized in the symmetric region of the parameter space. However, the transition appears to be sharper for this set of runs: beyond a threshold value, $\mathrm{Fr} \simeq 0.13$, a robust equatorial jet is suddenly formed, and its amplitude is only slightly increased by further increasing Fr. A similar behaviour, with an even sharper transition, was found for another series of runs with ten times smaller Ro. To the best of our knowledge, the presence of a threshold in Fr for the equatorial jet formation was not noted in previous works on this subject.

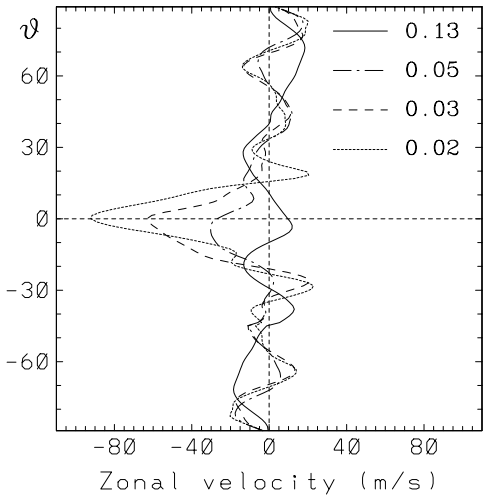

Fig. 2. – Steady-state meridional profiles of mean zonal velocity for different Rossby numbers $R_0 = (0.13, 0.05, 0.03, 0.02)$, at a fixed Froude number $Fr = 0.09$.

We find the threshold for equatorial jet formation to be very close to that for the breaking of cyclone-anticyclone symmetry. This correspondence is further qualified in ref. [11], where it is shown that the jet amplitude and the asymmetry index, defined as an extension to spherical geometry of the usual skewness factor, have similar dependences on Fr and similar time evolutions, suggesting the existence of a deep dynamical relation.

Here we only note that the direction and size of the equatorial jet is simply related to the global prevalence of one type of vorticity. This follows from Stokes's theorem applied to a given hemisphere, which allows to express the value of the zonal mean of

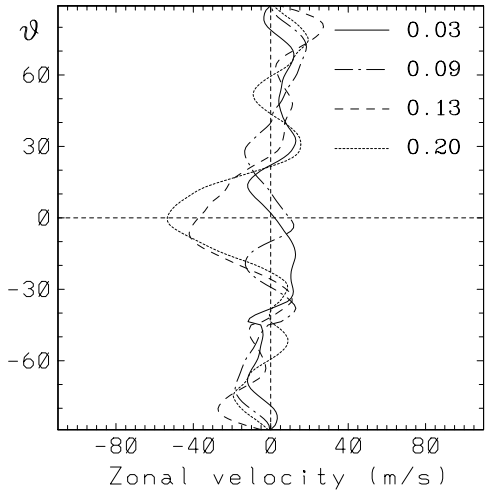

Fig. 3. – Steady-state meridional profiles of mean zonal velocity for different Froude numbers $Fr = (0.03, 0.09, 0.13, 0.2)$, at a fixed Rossby number $Ro = 0.13$.

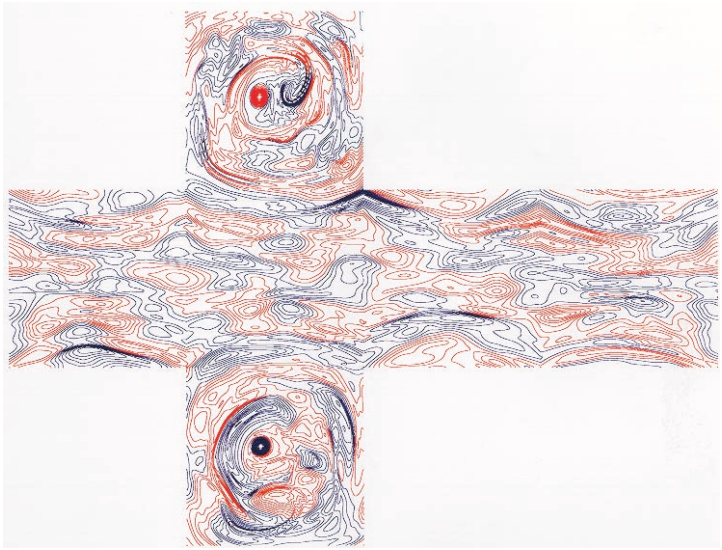

Fig. 4. – Relative vorticity field ζ after 560 planetary rotations, shown on the opened cubic computational domain (upper and lower panels centered on the North and South pole, respectively). The parameters of the run are Fr = 0.01 and Ro = 0.013. Negative (positive) values of ζ are plotted in blue (red).

the zonal velocity along the equator in terms of the integral of the relative vorticity ζ over the hemisphere under consideration (the same relation is obtained from the other hemisphere, since the integral of ζ over the entire spherical surface must vanish). As a

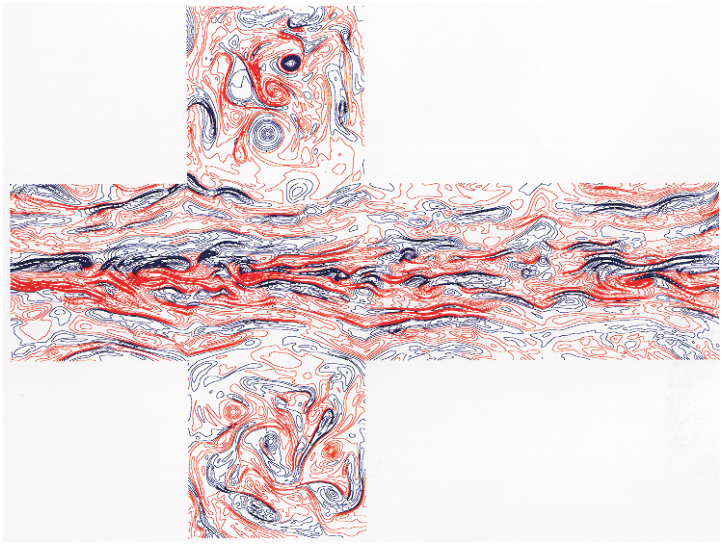

Fig. 5. – Same as in fig. 4, for a run with Fr = 0.055 and Ro = 0.013, which fall in the "asymmetric" region of the (Ro, Fr)-plane.

consequence, a westward (retrograde) equatorial jet must be associated with global prevalence of anticyclonic vorticity, *i.e.*, of vorticity of negative sign in the Northern hemisphere and of positive sign in the Southern one. By the same argument, a global dominance of cyclonic vorticity would lead to the formation of an eastward equatorial jet. This is just a general property of two-dimensional flows in spherical geometry; the role of shallow-water dynamics is that of allowing the prevalence of anticyclonic vorticity (steady states with a prevalence of cyclones were never found in our simulations or in those of ref. [7]).

To give a measure of how different the final states of the shallow-water evolution can be when starting from different sides of the threshold, we show in figs. 4 and 5 the steady-state relative vorticity fields for a "symmetric" run, with $\mathrm{Ro} = 0.013$, $\mathrm{Fr} = 0.01$, and for an "asymmetric" one, with $\mathrm{Ro} = 0.013$, $\mathrm{Fr} = 0.055$ (close to Jupiter parameters). The isolines of positive (negative) ζ are drawn in red (blue) on the global CS computational domain, which is shown opened on the plane. Note that in these figures the equator is a straight line cutting horizontally the computational domain in two equal halves. It can be seen in fig. 5 how, as a consequence of a process of reorganization of the flow around the equator, two bands of relative vorticity have been formed, with predominance of negative (positive) vorticity above (below) the equatorial line. Correspondingly, a robust westward equatorial jet was formed, with a maximum strength of about 100 m/s, which is almost three times the r.m.s. of the initial velocity field.

5. – Conclusions

We have performed long-time simulations of freely decaying shallow-water dynamics on a rotating sphere, using a new efficient grid point numerical method that allows to reach very high spatial resolutions.

In agreement with ref. [7], we observe that the presence of a finite deformation radius allows the spontaneous formation of equatorial jets, always westerly directed in the simulations. In addition, we find that, at a fixed rotation rate, this process has a quite sharp threshold in Froude number, which is close to that indicated in [7] as a threshold for the breaking of cyclone-anticyclone symmetry.

We also point out, from basic properties of two-dimensional flows in spherical geometry, that there is direct correspondence between the westward (eastward) direction of the equatorial jet and the global prevalence of anticyclonic (cyclonic) vorticity. Shallow-water dynamics determines a reorganization of the vorticity field in the equatorial region that leads to the global prevalence of anticyclonic vorticity in the final states of the evolution.

The mechanism of formation of the asymmetry and its relevance to the dynamics of planetary atmospheres need to be further investigated.

REFERENCES

[1] YODEN S. and YAMADA M., *J. Atmos. Sci.*, **50** (1993) 631.
[2] NOZAWA T. and YODEN S., *Phys. Fluids*, **9** (1997) 2081.
[3] CUSHMAN-ROISIN B. and TANG B., *J. Phys Oceanogr.*, **20** (1990) 97.
[4] FARGE M. and SADOURNY R., *J. Fluid Mech.*, **206** (1990) 433.

[5] SPALL M. A. and MCWILLIAMS J. C., *Geophys. Astrophys. Fluid Dyn.*, **64** (1992) 1.
[6] POLVANI L. M., MCWILLIAMS J. C., SPALL M. A. and FORD R., *Chaos*, **4** (1994) 177.
[7] CHO J. Y.-K. and POLVANI L., *Phys. Fluids*, **8** (1996) 1531.
[8] CHO J. Y.-K. and POLVANI L., *Science*, **273** (1996) 335.
[9] RONCHI C., IACONO R. and PAOLUCCI P. S., *Proceedings, HPCN Europe '95, Milan, Italy, May 3-5 1995*, in *Lecture Notes in Computer Science*, edited by G. GOOS, J. HARTMANIS and J. VAN LEEUWEN (Springer-Verlag).
[10] RONCHI C., IACONO R. and PAOLUCCI P. S., *J. Comput. Phys.*, **124** (1996) 93.
[11] IACONO R., STRUGLIA M. V. and RONCHI C., *Phys. Fluids*, **11** (1999) 1272.
[12] STARIUS G., *Numer. Math.*, **35** (1980) 241.
[13] DURRAN D., *Mon. Weather Rev.*, **119** (1991) 702.
[14] RONCHI C., IACONO R., STRUGLIA M. V., ROSSI A., TRUINI C., PAOLUCCI P. S. and PRATESI S., in *Parallel Computational Fluid Dynamics*, edited by P. SCHIANO *et al.* (Elsevier) 1997.
[15] BARTOLONI A. and THE APE GROUP, *Int. J. Mod. Phys. C*, **4** (1993) 955.
[16] BROWNING G. L., HACK J. J. and SWARZTRAUBER P. N., *Mon. Weather Rev.*, **117** (1989) 1058.